

AD-A078 157

NAVAL POSTGRADUATE SCHOOL MONTEREY CA
DYNAMIC STRUCTURAL MODEL OF A SUBMERGED RING.(U)
SEP 79 J T WALLER

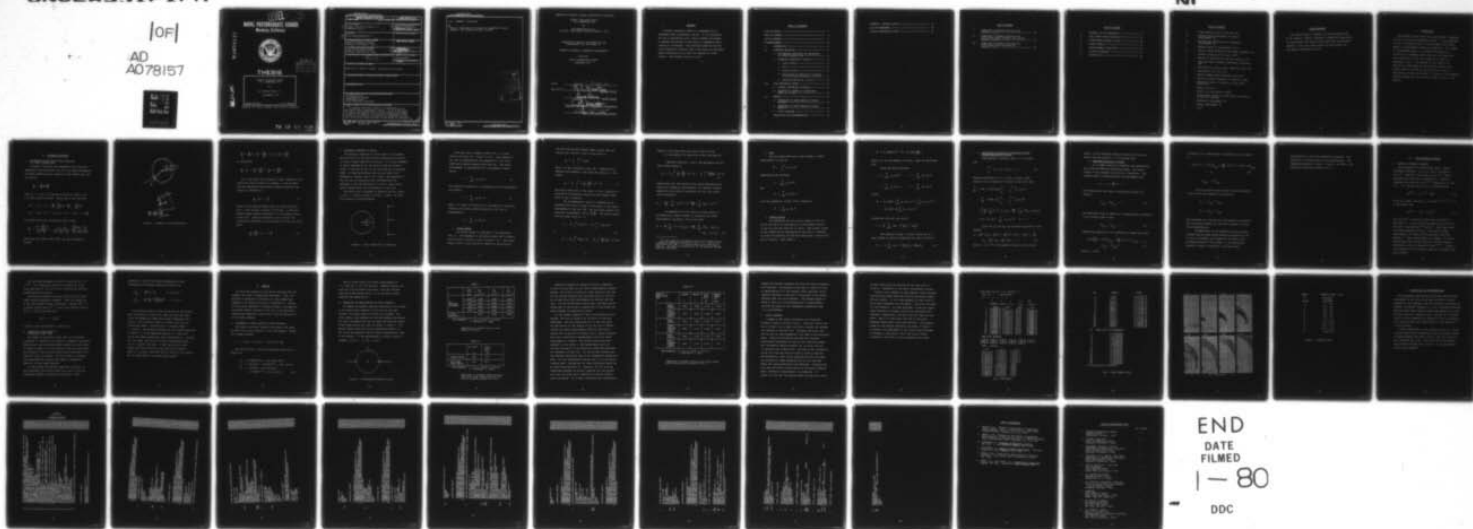
F/G 13/10

UNCLASSIFIED

NI

10F

AD
A078157



LEVEL 4

(2)

NAVAL POSTGRADUATE SCHOOL

Monterey, California

AD A078157



DDC
RECEIVED
DEC 14 1979
A

THESIS

DYNAMIC STRUCTURAL MODEL
OF A SUBMERGED RING

by

Jack Thomas Waller Jr.

September 1979

Thesis Advisor:

R. E. Newton

Approved for public release; distribution unlimited.

DDC FILE COPY

79 12 12 026

UNCLASSIFIED

SECURITY CLASSIFICATION OF THIS PAGE (When Data Entered)

REPORT DOCUMENTATION PAGE		READ INSTRUCTIONS BEFORE COMPLETING FORM
1. REPORT NUMBER	2. GOVT ACCESSION NO.	3. RECIPIENT'S CATALOG NUMBER
4. TITLE (and Subtitle) Dynamic Structural Model of a Submerged Ring		5. TYPE OF REPORT & PERIOD COVERED Master's Thesis September 1979
7. AUTHOR(s) Jack Thomas/Waller, Jr.		6. PERFORMING ORG. REPORT NUMBER
9. PERFORMING ORGANIZATION NAME AND ADDRESS Naval Postgraduate School Monterey, California 93940		8. CONTRACT OR GRANT NUMBER(s)
11. CONTROLLING OFFICE NAME AND ADDRESS Naval Postgraduate School Monterey, California 93940		10. PROGRAM ELEMENT, PROJECT, TASK AREA & WORK UNIT NUMBERS
14. MONITORING AGENCY NAME & ADDRESS (if different from Controlling Office) (12) 542		12. REPORT DATE Sep 1979
		13. NUMBER OF PAGES 50
		15. SECURITY CLASS. (of this report) Unclassified
		16a. DECLASSIFICATION/DOWNGRADING SCHEDULE
16. DISTRIBUTION STATEMENT (of this Report) Approved for public release; distribution unlimited.		
17. DISTRIBUTION STATEMENT (of the abstract entered in Block 20, if different from Report)		
18. SUPPLEMENTARY NOTES		
19. KEY WORDS (Continue on reverse side if necessary and identify by block number) Structural Ring Trigonometric Series Underwater Shock Fluid Structure Interface		
20. ABSTRACT (Continue on reverse side if necessary and identify by block number) A dynamic structural model of a submerged ring is developed using trigonometric series. It is constructed for use in conjunction with a finite element fluid model to examine the effects of cavitation on underwater shock loading of a structure. The governing equations and the time integration algorithm used in the model are described.		

DD FORM 1473
1 JAN 73
(Page 1)EDITION OF 1 NOV 65 IS OBSOLETE
S/N 0102-014-6601

1

UNCLASSIFIED 252 450
SECURITY CLASSIFICATION OF THIS PAGE (When Data Entered)

UNCLASSIFIED

SECURITY CLASSIFICATION OF THIS PAGE(When Data Entered)

(20. ABSTRACT Continued)

Results predicted by the model are compared to known results. The program listing is given.

Accession For	
NTIS GARRI	<input checked="" type="checkbox"/>
DOC TAB	<input type="checkbox"/>
Unannounced	<input type="checkbox"/>
Classification	<input type="checkbox"/>
By	
Distribution/	
Availability Codes	
Dist	Avail and/or special
A	

DD Form 1473
1 Jan 73
S/N 0102-014-6601

UNCLASSIFIED

SECURITY CLASSIFICATION OF THIS PAGE(When Data Entered)

Approved for public release; distribution unlimited.

Dynamic Structural Model
of a Submerged Ring

by

Jack Thomas Waller Jr.
B.S.M.E., New Mexico State University, 1975

Submitted in partial fulfillment of the
requirements for the degree of

MASTER OF SCIENCE IN MECHANICAL ENGINEERING

from the

NAVAL POSTGRADUATE SCHOOL
September 1979

Author

Jack T. Waller Jr.

Approved by:

R. E. Newton

Thesis Advisor

David Salinas

Second Reader

H. J. Marks

Chairman, Department of Mechanical Engineering

William M. Jolley

Dean of Science and Engineering

ABSTRACT

A dynamic structural model of a submerged ring is developed using trigonometric series. It is constructed for use in conjunction with a finite element fluid model to examine the effects of cavitation on underwater shock loading of a structure. The governing equations and the time integration algorithm used in the model are described. Results predicted by the model are compared to known results. The program listing is given.

TABLE OF CONTENTS

LIST OF TABLES -----	7
LIST OF FIGURES -----	8
LIST OF SYMBOLS -----	9
ACKNOWLEDGEMENT -----	10
I. INTRODUCTION -----	11
II. GOVERNING EQUATIONS -----	12
A. DIFFERENTIAL EQUATIONS FOR DEFLECTION OF A THIN CIRCULAR RING -----	12
B. GOVERNING EQUATIONS OF MOTION -----	15
1. Strain Energy -----	16
2. Work -----	19
3. Kinetic Energy -----	19
4. Application of Hamilton's Principle to Find Coupled Equations of Motion --	21
5. Separated Equations of Motion -----	22
III. TIME INTEGRATION METHOD -----	25
A. CENTRAL DIFFERENCE ALGORITHM -----	25
B. SELECTION OF NUMBER OF VIBRATIONAL MODES TO BE USED -----	26
IV. RESULTS -----	28
A. COMPARISON OF MODEL RESULTS TO EXACT SOLUTION -----	28
B. COMPARISON OF MODEL RESULTS TO STATIC BEHAVIOR -----	29
C. OUTPUT EXAMPLES -----	33
V. CONCLUSIONS AND RECOMMENDATIONS -----	39

APPENDIX: PROGRAM LISTING -----	40
LIST OF REFERENCES -----	49
INITIAL DISTRIBUTION LIST -----	50

LIST OF TABLES

I.	Comparison of program solution with analytic solution -----	30
II.	Comparison of dynamic solution with twice known static solution for uniform external pressure on ring -----	30
III.	Comparison of dynamic solution with twice known static solution for loading of Fig. 3 -----	32

LIST OF FIGURES

1.	Geometry of Ring Deformation -----	13
2.	Ring, Shock Front Orientation -----	15
3.	Concentrated Loading on Ring -----	29
4.	Output Example -----	35
5.	Output Example (Continued) -----	36
6.	Cavitation Example -----	37
7.	Pressure Code -----	38

LIST OF SYMBOLS

A	- cross sectional area of the ring (m^2)
a_n	- Fourier cosine coefficient for radial displacement (m)
b_n	- Fourier sine coefficient for tangential displacement (m)
c	- speed of sound in ring material (m/s)
c_n	- Fourier cosine coefficient for normal pressure (Pa)
D	- flexural rigidity of the ring ($N \cdot m^2$)
E	- modulus of elasticity of the ring material (Pa)
h	- time step used in central difference integration (sec)
I	- area moment of inertia about centroidal axis (m^4)
κ	- curvature of the ring (1/m)
M	- bending moment about centroidal axis ($N \cdot m$)
ω_n	- natural circular frequency of vibration (rad/s)
r	- centroidal radius of gyration of ring cross section (m)
R	- radius of ring (m)
ρ	- density of ring material (kg/m^3)
θ	- angle between normal to shock plane and location on the ring (radians)
v	- tangential displacement (m)
w	- radial displacement (m)
z	- $(r/R)^2$

ACKNOWLEDGEMENT

The author wishes to express his sincere appreciation to Dr. Robert E. Newton, Professor of Mechanical Engineering, for his patience and guidance which made this investigation possible. Also, the author thanks his wife, Belen, for her support throughout his work.

I. INTRODUCTION

The program evolved during this study models a submerged circular ring using trigonometric series. It was developed for use in conjunction with a finite element fluid model based on a displacement potential formulation. The purpose of the combined models is to predict the effects of cavitation on underwater shock loading of the structure. More information on the fluid model can be found in References 1 and 2. The purpose of this paper is to describe the development of the structural model and to present some of the results obtained from its use in combination with the fluid model. A listing of the FORTRAN IV program implementing the structural model is given in the Appendix.

II. GOVERNING EQUATIONS

A. DIFFERENTIAL EQUATIONS FOR THE DEFLECTION OF A THIN CIRCULAR RING

In Figure 1 the solid line represents the ring after deformation, and the dotted line the ring before deformation. For small deflections the curvature of the element m_1n_1 can be taken as

$$\frac{1}{R_1} = \frac{d\theta + \Delta d\theta}{ds + \Delta ds}$$

where R , w , θ and s are defined as shown in Figure 1 and w is taken positive inward. Making use of the relations

$$\Delta d\theta = d\theta_1 - d\theta = \frac{dw}{ds} + \frac{d^2w}{ds^2} ds - \frac{dw}{ds} = \frac{d^2w}{ds^2} ds$$

$$\Delta ds = ds_1 - ds = (r-w)d\theta - rd\theta = -wd\theta = -w \frac{ds}{R}$$

and substituting into the equation above yields

$$\frac{1}{R_1} = \frac{d\theta + \frac{d^2w}{ds^2} ds}{ds(1 - \frac{w}{R})} = \frac{d\theta(1 + \frac{w}{R})}{ds(1 - \frac{w}{R})(1 + \frac{w}{R})} + \frac{\frac{d^2w}{ds^2} ds(1 + \frac{w}{R})}{ds(1 - \frac{w}{R})(1 + \frac{w}{R})}$$

Neglecting the higher order terms, the above expression becomes

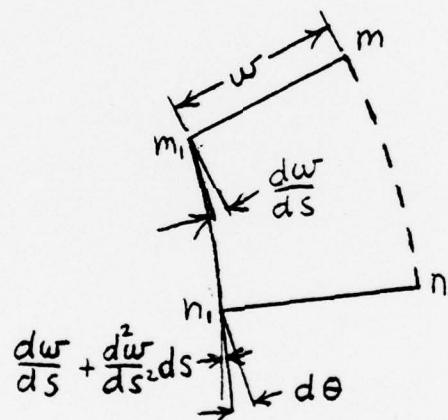
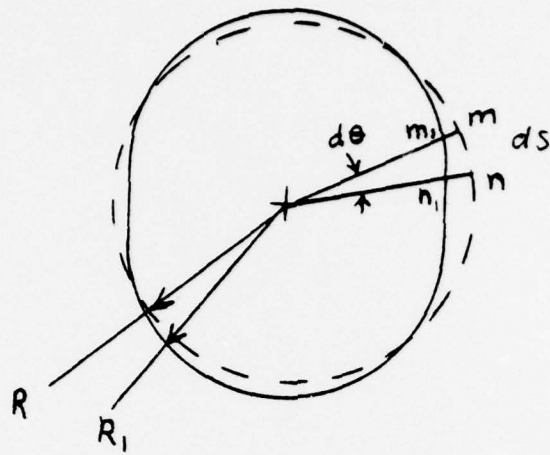


Figure 1. Geometry of Ring Deformation

$$\frac{1}{R_1} = \frac{d\theta}{ds} \left(1 + \frac{w}{R}\right) + \frac{d^2 w}{ds^2} = \frac{1}{R} \left(1 + \frac{w}{R}\right) + \frac{d^2 w}{ds^2}$$

or alternately

$$\frac{1}{R_1} - \frac{1}{R} = \frac{w}{R^2} + \frac{d^2 w}{ds^2} = \frac{1}{R^2} \left(w + \frac{d^2 w}{d\theta^2}\right) \quad (1)$$

For a ring where the thickness is small compared to the radius and elastic behavior is assumed, it can be shown that the approximate relationship between deflection and loading is [Reference 7]

$$\frac{1}{R_1} - \frac{1}{R} = - \frac{M}{D} \quad (2)$$

where M is the bending moment about the centroidal axis and D is the flexural rigidity of the ring. A positive bending moment produces compression in the outside fibers of the ring. Combining equations 1 and 2 yields the differential equations for the deflection of the ring given below.

$$\frac{1}{R^2} \left(\frac{\partial^2 w}{\partial \theta^2} + w\right) = - \frac{M}{D} \quad (3)$$

B. GOVERNING EQUATIONS OF MOTION

The governing equations of motion used in the program were arrived at by the application of Hamilton's principle. In order to apply Hamilton's principle, it is first necessary to derive expressions for the strain energy and kinetic energy of the ring as well as the work done by the external loads. In these derivations the ring was taken to be homogeneous, elastic, and of unit width. The pressures on the ring and its deflection were represented by the pressures at and the deflection of a set of nodal points equally spaced along the circumference of the ring.

The shock front is assumed to approach the ring normal to the $\theta = 0$ plane as shown in Figure 2, where θ is taken to be positive counterclockwise.

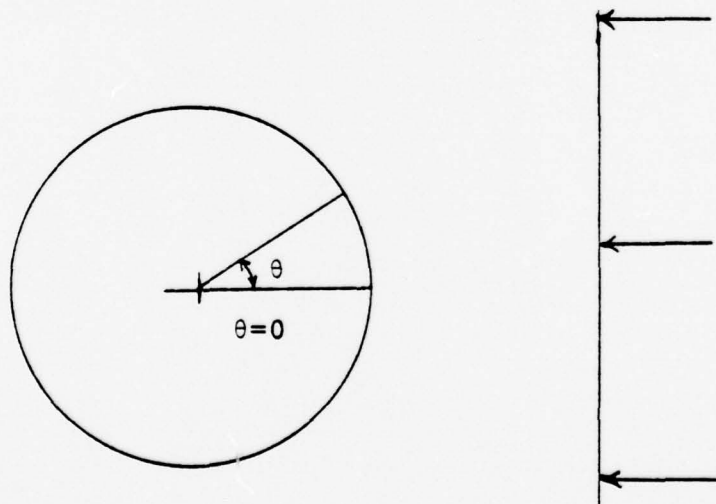


Figure 2. Ring, Shock Front Orientation

Since the ring is symmetric about the $\theta = 0$ plane, results are given for θ from 0° to 180° . The response of the ring is represented by the response of a set of $N+1$ nodal points equally spaced along the ring. The radial displacement is approximated by a trigonometric cosine series

$$w = \sum_{n=0}^N a_n \cos n\theta \quad . \quad (4)$$

The tangential deflection is represented by the trigonometric sine series

$$v = \sum_{n=1}^N b_n \sin n\theta \quad , \quad (5)$$

where v is taken to be positive in the negative θ direction. Similarly the normal pressure applied to the ring is represented by

$$p = \sum_{n=0}^N c_n \cos n\theta \quad . \quad (6)$$

1. Strain Energy

The strain energy is comprised of two components [Ref. 4]. One component is the strain energy due to bending and the other to strain in the θ direction (ϵ_θ). The strain energy stored in the ring due to bending is calculated as

the work done by the internal moment acting over the entire ring, and for a ring of unit width is

$$U_B = \frac{1}{2} \int_0^{2\pi} M R \kappa d\theta$$

where κ is the curvature of the ring. Combining this equation with equation 3 and using the relation $\kappa = M/D$ yields

$$U_B = \frac{1}{2} \int_0^{2\pi} D \frac{1}{R^3} \left(\frac{\partial^2 w}{\partial \theta^2} + w \right)^2 d\theta \quad (7)$$

The strain energy due to the strain in the θ direction is obtained as the distance traveled by the average normal force in the θ direction.

The circumferential strain is composed of two components the first of which is the result of the radial displacement of the ring ($\frac{w}{R}$) and the second results from tangential displacement and is ($\frac{1}{R} \frac{\partial v}{\partial \theta}$). The strain energy from the normal force (N) is

$$U_\theta = \frac{1}{2} \int_0^{2\pi} N \epsilon_\theta R d\theta = \frac{1}{2} \int_0^{2\pi} A \epsilon_\theta E \epsilon_\theta R d\theta$$

or

(8)

$$U_\theta = \frac{1}{2} \int_0^{2\pi} R A E \epsilon_\theta^2 d\theta = \frac{1}{2} \int_0^{2\pi} \frac{A E}{R^2} \left(\frac{\partial v}{\partial \theta} + w \right)^2 R d\theta$$

where A is the cross sectional area of the ring and

E is the modulus of elasticity of the ring material.

Combining equations 7 and 8, the expression for the total strain energy is

$$U_T = \frac{1}{2} \int_0^{2\pi} \frac{D}{R^3} \left(\frac{\partial^2 w}{\partial \theta^2} + w \right)^2 d\theta + \frac{1}{2} \int_0^{2\pi} \frac{AE}{R} \left(\frac{\partial v}{\partial \theta} + w \right)^2 d\theta \quad (9)$$

Substituting into this equation the series expressions for radial and tangential displacements, and assuming constant geometrical and material properties over the ring yields after integration

$$U_T = \frac{\pi D}{2R^3} \left[\sum_{n=0}^N a_n^2 (n^2 - 1)^2 + \frac{AE\pi}{2R} \left[\sum_{n=0}^N (nb_n + a_n)^2 \right] \right]^* \quad *$$

An expression for the change in strain energy δU corresponding to small changes in tangential and radial displacements (δb_n and δa_n) can now be found

$$\delta U = \frac{\pi D}{3} \left[\sum_{n=0}^N (n^2 - 1)^2 a_n \delta a_n \right] + \frac{AE\pi}{R} \left[\sum_{n=0}^N (n^2 b_n + na_n) \delta b_n + (nb_n + a_n) \delta a_n \right] \quad (10)$$

* In this equation and several that follow which contain a summation expression starting with $n = 0$, a factor of 2 associated with the $n = 0$ term is omitted for the sake of brevity. The term is accounted for in the solution process used with the model.

2. Work

The work associated with a small change in radial displacement is given by

$$\delta W = \int_0^{2\pi} p \delta w R d\theta$$

Substituting the relations

$$p = \sum_{m=0}^N c_m \cos m\theta$$

and

$$\delta w = \sum_{n=0}^N \delta a_n \cos n\theta$$

into this expression yields, after integration

$$\delta W = \sum_{n=0}^N c_n \delta a_n \pi R$$

3. Kinetic Energy

The expression for the kinetic energy of the ring can be arrived at by considering an infinitesimal section of the ring that has been set in motion. The kinetic energy of the element can be represented as the sum of a contribution due to translation of the mass center and a contribution due to rotation. This leads to

$$dT = \frac{1}{2} \rho (AR d\theta) (\dot{w}^2 + \dot{v}^2) + \frac{1}{2} \rho IR d\theta \left(\frac{\partial \dot{w}}{R \partial \theta} \right)^2$$

where I is the area moment of inertia about the centroidal axis.

Using the series relations

$$w = \sum_{n=0}^N a_n \cos n\theta \quad \dot{w} = \sum_{n=0}^N \dot{a}_n \cos n\theta$$

$$v = \sum_{n=1}^N b_n \sin n\theta \quad \dot{v} = \sum_{n=1}^N \dot{b}_n \sin n\theta$$

yields

$$dT = \frac{1}{2} \rho (AR d\theta) \left[\left(\sum_{n=0}^N \dot{a}_n \cos n\theta \right)^2 + \left(\sum_{n=1}^N \dot{b}_n \sin n\theta \right)^2 \right] \\ + \frac{1}{2} \rho IR d\theta \left(-\frac{1}{R} \sum_{n=1}^N \dot{a}_n n \sin n\theta \right)^2$$

Integration over the ring yields

$$T = \frac{\pi \rho}{2} \sum_{n=0}^N \left[\left(AR + n^2 \frac{I}{R} \right) \dot{a}_n^2 + AR \dot{b}_n^2 \right]$$

The resultant change in kinetic energy due to a small change in velocity components can then be found as

$$\delta T = \pi \rho \sum_{n=0}^N \left[\left(AR + n^2 \frac{I}{R} \right) \dot{a}_n \delta \dot{a}_n + AR \dot{b}_n \delta \dot{b}_n \right] \quad (12)$$

4. Application of Hamilton's Principle To Find Coupled Equations of Motion

From Hamilton's principle [Ref. 5] it is known that

$$\int_{t_1}^{t_2} (\delta T - \delta U + \delta W) dt = 0 \quad (13)$$

Combining equations 10, 11, 12 and 13 yields, after carrying out an integration by parts on the first term,

$$\begin{aligned} & \sum_{n=0}^N \pi \rho (AR + n^2 \frac{I}{R}) [\dot{a}_n \delta a_n]_{t_1}^{t_2} - \int_{t_1}^{t_2} \ddot{a}_n \delta a_n dt \\ & + \sum_{n=0}^N \pi \rho AR [\dot{b}_n \delta b_n]_{t_1}^{t_2} - \int_{t_1}^{t_2} \ddot{b}_n \delta b_n dt \\ & - \int_{t_1}^{t_2} \left\{ \frac{\pi D}{R^3} \left[\sum_{n=0}^N (n^2 - 1)^2 a_n \delta a_n \right] + \frac{AE\pi}{R} \left[\sum_{n=0}^N (n^2 b_n + n a_n) \delta b_n \right. \right. \\ & \left. \left. + (n b_n + a_n) \delta a_n \right] - \sum_{n=0}^N c_n \delta a_n \pi R \right\} dt = 0 \end{aligned}$$

Since the δa_n and δb_n can be chosen arbitrarily, this becomes

$$\begin{aligned} (1 + (\frac{r}{R})^2 n^2) \ddot{a}_n + (\frac{c}{R})^2 [1 + (\frac{r}{R})^2 (n^2 - 1)^2] a_n + (\frac{c}{R})^2 &= \frac{c_n}{\rho A} \\ \ddot{b}_n + (\frac{c}{R})^2 n a_n + (\frac{c}{R})^2 n^2 b_n &= 0 \end{aligned} \quad (14)$$

where $c = (E/\rho)^{1/2}$ is the speed of sound in the ring and

where r is the centroidal radius of gyration of the ring section and the relation $I = Ar^2$ has been used.

5. Separated Equations of Motion

It is common practice to separate ring deformations into flexural modes and extensional modes. The initial version of this program utilized such a resolution. The flexural mode is characterized by the requirement that

$$\epsilon_{\theta} = - (w + \frac{\partial v}{\partial \theta})/R = 0 .$$

This implies that the Fourier coefficients satisfy the relation

$$a_{n(F)} + nb_{n(F)} = 0 \quad (15)$$

The extensional mode is defined to be geometrically orthogonal to the flexural mode so that

$$na_{n(E)} - b_{n(E)} = 0 \quad (16)$$

Substituting equation 15 into equations 14 yields the result

$$\begin{aligned} [\rho A (\frac{n^2+1}{n^2}) + zn^2] \ddot{a}_{n(F)} + [\frac{EA}{R^2} z (n^2-1)^2] a_{n(F)} &= c_n \\ b_{n(F)} &= -a_{n(F)}/n \end{aligned} \quad (17)$$

where $z = (r/R)^2$.

If equation 16 is substituted into equations 14, the result is

$$[\rho A((n^2 + 1) + zn^2)]\ddot{a}_{n(E)} + \left[\frac{EA}{R^2}((n^2 + 1)^2 + z(n^2 - 1)^2)\right]a_{n(E)} = c_n \quad (18)$$

$$b_{n(E)} = na_{n(E)}$$

Initial solutions were carried out using equations 17 and 18 and then combining the results by

$$a_n = a_{n(F)} + a_{n(E)}$$

$$b_n = b_{n(F)} + b_{n(E)}$$

This procedure gave results which satisfactorily predicted the ring bending moments but gave poor accuracy for axial force determinations.

Re-examination of the foregoing solution process revealed that the mode shapes defined by equations 15 and 16 are not orthogonal with respect to the mass or the stiffness matrices of the system. It was accordingly decided to return to equations 14 and solve them

simultaneously in the time integration algorithm. This change led to accurate axial force determinations. The separated equations of motion, 17 and 18, are used in the program as described in Section III, b.

III. TIME INTEGRATION METHOD

A. CENTRAL DIFFERENCE ALGORITHM

Time integration is accomplished using a central difference algorithm. If a_n , b_n , and c_n are known at time $t^{(i)}$, then $\ddot{a}_n^{(i)}$ (the value of \ddot{a}_n at $t^{(i)}$) may be evaluated from the first of equations 14. Letting h represent the time step and $\dot{a}_n^{(i-\frac{1}{2})}$ represent \dot{a}_n at time $t^{(i)} - h/2$, the next value of \dot{a}_n is calculated from

$$\dot{a}_n^{(i+\frac{1}{2})} = \dot{a}_n^{(i-\frac{1}{2})} + h\ddot{a}_n^{(i)} \quad (19)$$

Using this result, the next a_n (at time $t^{(i+1)} = t^{(i)} + h$) is calculated from

$$a_n^{(i+1)} = a_n^{(i)} + h\dot{a}_n^{(i+\frac{1}{2})} \quad (20)$$

The value $\ddot{b}_n^{(i)}$ is similarly found from the second of equations 14. A pair of equations paralleling 19 and 20 are used to calculate $\dot{b}_n^{(i+\frac{1}{2})}$ and $b_n^{(i+1)}$. When these steps have been completed for each n , the value of radial displacement w is found at each structural node from equation 4. These displacements are passed to the fluid program where they furnish required interface boundary conditions to allow an advance to time $t^{(i+1)}$. Values of fluid pressure at the interface nodes are returned by the fluid program.

The new nodal pressures are used to calculate c_n 's at $t^{(i+1)}$. It is then again possible to advance \dot{a}_n and a_n using equations 14, 19, and 20 and to perform the parallel calculations for \dot{b}_n and b_n .

The solution process is started with the ring at rest under uniform hydrostatic pressure. Under the loading a_0 is the only nonzero Fourier coefficient. Because $\dot{a}_n^{(0)} = 0$ is known (rather than $\dot{a}_n^{(-\frac{1}{2})}$), a fictitious starting value of $\dot{a}_n^{(-\frac{1}{2})}$ is first calculated from

$$\dot{a}_n^{(-\frac{1}{2})} = -\frac{h}{2} \ddot{a}_n^{(0)}$$

A similar starting procedure is used for \dot{b}_n .

B. SELECTION OF THE NUMBER OF VIBRATIONAL MODES USED

The number of vibrational modes that can be modeled accurately is limited by the numerical integration algorithm. Specifically, the algorithm becomes unstable for time steps in excess of about 0.3 of the period of the structural mode. The accuracy of the algorithm deteriorates even before the stability limit is reached. For this reason, a criterion was established for limiting the number of modes used, based on the time steps selected.

In the program the separated equations of motion for the extensional and flexural modes were used to find the frequencies needed in applying the criterion. From

equations 17 and 18 the natural frequencies of the extensional and flexural modes were found to be

$$\omega_{n(E)}^2 = \left(\frac{C}{R}\right)^2 (1 + n^2) \quad n = 0, 1, 2, 3, \dots$$

$$\omega_{n(F)}^2 = \left(\frac{C}{R}\right)^2 \left(\frac{r}{R}\right)^2 \frac{n^2 (n^2 - 1)^2}{n^2 + 1} \quad n = 2, 3, 4, \dots$$

The criterion used was that the period for the highest mode retained be at least five times the time step used. Since the extensional modes have higher frequencies for a given n , this criterion comes into effect first for the extensional modes. Once the point is reached (where $n = n_E(\text{max})$), the program switches from the coupled equations of motion 14, to the separated equation 17. When this occurs the higher extensional mode coefficients ($n > n_E(\text{max})$) are not needed, and only the flexural mode coefficients (for $n > n_E(\text{max})$) are used. If the time step is large enough that the criterion is also met by the flexural modes ($n = n_F(\text{max})$) then both the a_n 's and b_n 's are omitted for all modes where n is greater than $n_F(\text{max})$.

IV. RESULTS

To check the accuracy of the results obtained from the program, two kinds of comparisons were made. First, the solution of equations 14 arrived at by the program were compared to an analytic solution of equations 14. Second, to verify that equations 14 correctly predict ring behavior, calculated dynamic response of the ring to two particular loadings was compared to known static results [Reference 6] for the same loadings.

A. COMPARISON OF MODEL RESULTS TO EXACT SOLUTION

The check on solution accuracy was based on the exact solution for a ring initially at rest and suddenly loaded by a steady pressure

$$P = [1.625 - .25 \cos \theta - .375 \cos 2\theta] \text{ MPa}$$

The exact solution, using the parameters specified in Table I, is

$$\begin{aligned} a_0 &= 4.05844 \times 10^{-3} [1 - \cos (1011.303t)] \\ a_1 &= -159.483t^2 - 1.5617 \times 10^{-4} [1 - \cos (1429.t)] \\ a_2 &= -.104129 [1 - \cos (85.616)t] \\ &\quad - 3.7355 \times 10^{-5} [1 - \cos (2259.7t)] \end{aligned} \quad (22)$$

Table I gives results for radial displacements at $t = 1$ msec for $\theta = 0^\circ$, 90° and 180° . Computer results are given for four different time steps. Even the coarsest time step gives results within 1% of the exact values obtained from equations 22.

B. COMPARISON OF MODEL RESULTS TO STATIC BEHAVIOR

To compare the dynamic response predicted by the program to the known static response of the ring for the same loading, two simple cases of loading were assumed. The first loading case examined was uniform pressure surrounding the ring; the second case was two equal and opposite concentrated loads acting 180° apart as shown in Figure 3. The second loading case could not be represented exactly by the finite trigonometric series loading representation used by the program. It was approximated by nonzero values of pressure only at $\theta = 0^\circ$ and $\theta = 180^\circ$.

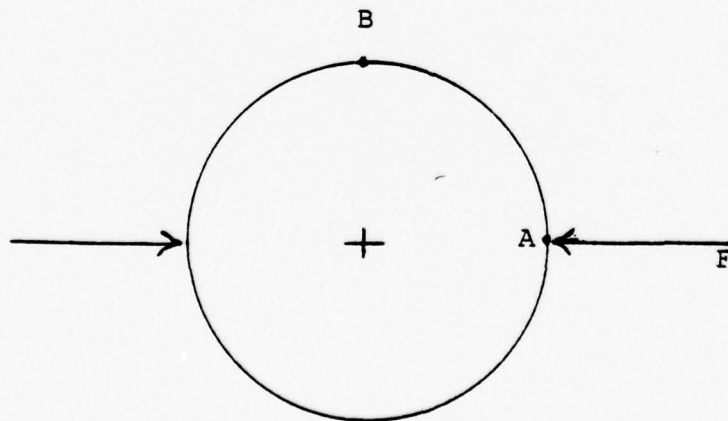


Figure 3. Concentrated Loading on Ring

TABLE I

	Time Step sec	ΔR NP1 $m \times 10^{-7}$	ΔR NP2 $m \times 10^{-7}$	ΔR NP3 $m \times 10^{-7}$
ΔR predicted by program	2.5×10^{-4}	11619.	23687.	17556.
	1×10^{-5}	11679	23472.	17553
	1×10^{-6}	11682	23469.	17555.
	1×10^{-7}	11683.	23469.	17555.
ΔR from equations 17		11683.	23469.	17555.

Ring Parameters: $R = 5 \text{ m}$, $A = .05 \text{ m}^2$, $E = 200 \text{ GPa}$
 $\rho = 7830 \text{ kg/m}^3$, $r = .158 \text{ m}$

Comparison of program solution with
analytic solution

TABLE II

	ΔR (max) mm	Axial Force (Max) MN
Program results	4.98	-9.8
Twice Known Static Results	5.00	-10.0

Ring Parameters: $R = 5 \text{ m}$, $A = .05 \text{ m}^2$, $E = 200 \text{ GPa}$
 $\rho = 7830 \text{ kg/m}^3$, $r = .158 \text{ m}$

Comparison of program dynamic solution
with twice known static solution for
uniform external pressure on ring

Comparison between the dynamic and static responses of the ring were made for the radial displacements, bending moments, and forces at particular nodal points on the ring. For the uniform pressure case any nodal point on the ring can be used since the displacements are uniform over the ring. For the concentrated loading case, the nodal points chosen were at the points of application of the forces and midway between the application points.

For the dynamic response of the ring predicted by the program, the ring is taken to be initially at rest and undeformed. The anticipated behavior of the ring after the application of the loading is for the ring to deflect through the radial displacements found for the static loading and to continue to deflect until a radial displacement with a magnitude of approximately twice the static displacement is reached. The maximum deflections were expected to occur after a time approximately equal to one half the period of the vibrational mode that dominates the deflection of the ring. For the uniform loading case the dominant vibrational mode is the fundamental extensional mode. For the concentrated loading case, it is the second flexural mode. The periods for these vibrational modes can be found using equations 21. Tables II and III give the comparisons between the dynamic response from the program and twice the known static response for the two loading cases considered. As is seen, relatively good correlations

TABLE III

Number of Nodal Points Used		ΔR_A (max) m	ΔR_B (max) m	Axial Force at B MN	Bending Moment at B MN.m
5	Model Results	.2965	-.2839	-3.760	-7.910
	Static Analysis Results Times 2	.2634	-.2421	-3.536	-6.434
7	Model Results	.2013	-.1857	-2.353	-4.737
	Static Analysis Results Times 2	.1862	-.1713	-2.500	-4.543
9	Model Results	.1510	-.1393	-1.743	-3.544
	Static Analysis Results Times 2	.1425	-.1311	-1.913	-3.477

Ring Parameters: $R = 5 \text{ m}$, $A = .05 \text{ m}^2$, $E = 200 \text{ GPa}$
 $\rho = 7830 \text{ kg/m}^3$, $r = .158 \text{ m}$

Comparison of dynamic solution with twice known
static solution for loading of Fig. 3

between the dynamic responses and twice the static responses were obtained. The maximum values shown in Table III occur at approximately 35.3 milliseconds after time zero, which compares favorably to one half of the period of the second flexural mode (36.6 milliseconds). The maximum values in Table II occur at 3 milliseconds which is approximately one half the period of the fundamental extensional mode (3.11 milliseconds).

C. OUTPUT EXAMPLES

A sample of the output produced by the structural program is shown in Figures 4 and 5. The print code at the top of Figure 4 is an input code used to select the information desired in the print out. Following the print code are two sets of input parameters to be used in the structural model. These are followed by the mass and stiffness coefficients calculated for each of the vibrational modes. This information remains constant for any given run and is therefore only printed once. The rest of the information varies with time and can be printed as often as desired. The pressures at nodal points generated by the fluid model are printed out; these pressures are for one time step before the time printed below the pressures. Following the time come the Fourier coefficients for the radial displacements, tangential displacements, and pressures. In Figure 5 at the top, the bending moment and the axial force

at each nodal point are printed for the time given in Figure 4. Tabulation of the radial displacement follows.

Figure 6 is an example of the graphical output obtained from the fluid model when the fluid and structural models are run jointly. It is a time sequence of eight plots of fluid nodal pressures over the domain. The plots are shown at 8 ms intervals. The left hand edge of each plot represents the plane of symmetry and the top and bottom rows represent, respectively, the entry and exit faces for the shock. The x's on the lower left side of the plots represent dummy nodes inside the structure. The pressure ranges for the mapping characters are shown in Figure 7. In Figure 6 the development of the cavity can be followed. It develops in the second, third, and fourth frames, collapses in the fifth, and has vanished by the sixth.

PRINT CODE: 121111111 1 112 11415161718 1 1

NNEL NNP M N NNRAIN NNRAIN

16 17 2 0 9 17

	A	E	R	PI	RHO
	0.500D-01	0.200D 12	5.00	0.158	0.783D 04
I	XKAIN	XKREN	XKAIN	XKBIN	
1	0.40040D 09	0.0	391.50	0.0	
2	0.40000D 09	0.10217D 07	391.89	0.40000D 09	
3	0.40360D 09	0.20434D 07	393.07	0.80000D 09	
4	0.42560D 09	0.30651D 07	395.82	0.12000D 10	
5	0.49000D 09	0.40868D 07	397.76	0.16000D 10	
6	0.63040D 09	0.51086D 07	401.29	0.20000D 10	
7	0.89000D 09	0.61303D 07	405.59	0.24000D 10	
8	0.13216D 10	0.71520D 07	410.68	0.28000D 10	
9	0.19876D 10	0.81737D 07	416.56	0.32000D 10	
10	0.29600D 10	0.91954D 07	423.21	0.36000D 10	
11	0.43204D 10	0.10217D 08	430.65	0.40000D 10	
12	0.61600D 10	0.11239D 08	438.87	0.44000D 10	
13	0.85796D 10	0.12261D 08	447.88	0.48000D 10	
14	0.11690D 11	0.13282D 08	457.66	0.52000D 10	
15	0.15610D 11	0.14304D 08	468.23	0.56000D 10	
16	0.20470D 11	0.15326D 08	479.59	0.60000D 10	
17	0.26410D 11	0.16347D 08	491.72	0.64000D 10	

NODAL POINT PRESSURES

0.12D 08	0.98D 07	0.56D 07	0.21D 07	0.52D 06	0.23D 06
0.21D 06	0.20D 06	0.20D 06	0.20D 06	0.21D 06	0.21D 06
0.16D 06	0.20D 06	0.20D 06	0.20D 06	0.20D 06	0.20D 06

TIME = 0.250 MS

BN	AN	CN
0.0	0.59923D-03	0.16297D 07
-0.43636D-05	0.19121D-03	0.27357D 07
-0.76030D-05	0.16785D-03	0.23797D 07
-0.90953D-05	0.13425D-03	0.18891D 07
-0.87862D-05	0.98196D-04	0.13588D 07
-0.70533D-05	0.63913D-04	0.96420D 06
-0.48681D-05	0.37398D-04	0.48882D 06
-0.27813D-05	0.18732D-04	0.23172D 06
-0.11520D-05	0.89591D-05	76529.
-0.24755D-06	0.22288D-05	18334.
0.76762D-08	-0.76762D-07	-8451.9
0.70517D-07	-0.77569D-06	-15526.
0.11450D-07	-0.13740D-06	-4885.4
0.64630D-07	-0.84018D-06	-14242.
0.48881D-07	-0.68433D-06	-10788.
0.38325D-07	-0.57487D-06	-8187.1
0.33831D-07	-0.54130D-06	-9139.7

Fig. 4. Output Example

NP	MOMENT	FORCE
1	61466.	-0.22717D 07
2	38662.	-0.21430D 07
3	-31443.	-0.18193D 07
4	-46162.	-0.14334D 07
5	-27598.	-0.11448D 07
6	-7468.4	-0.18173D 07
7	-5001.3	-0.99940D 06
8	-5005.4	-0.10045D 07
9	-5152.0	-0.10006D 07
10	-4923.6	-0.99825D 06
11	-5237.5	-0.10017D 07
12	-3399.1	-0.10010D 07
13	-7444.2	-0.99792D 06
14	-3635.2	-0.99765D 06
15	-5265.8	-0.10009D 07
16	-4963.8	-0.99989D 06
17	-4983.9	-0.99806D 06

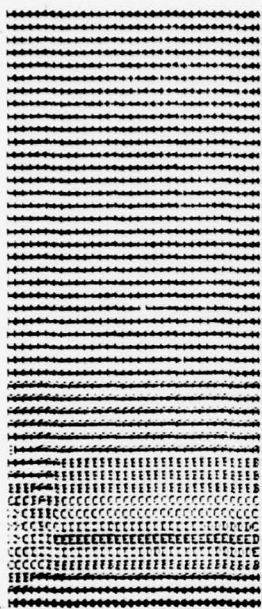
NP NODAL POINT DISPLACEMENTS

1	0.13157D-02
2	0.11784D-02
3	0.86677D-03
4	0.62037D-03
5	0.51822D-03
6	0.50099D-03
7	0.50035D-03
8	0.49977D-03
9	0.49981D-03
10	0.49984D-03
11	0.50032D-03
12	0.50019D-03
13	0.49695D-03
14	0.49935D-03
15	0.49947D-03
16	0.49921D-03
17	0.49944D-03

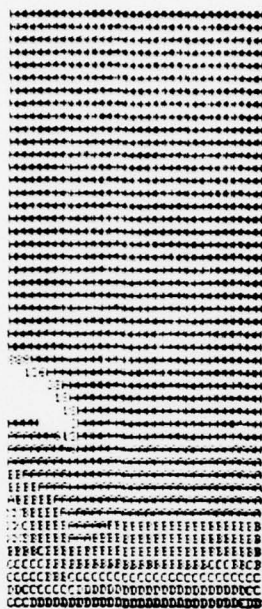
R: T=10.40/12.73 10.28.52

Fig. 5. Output Example (cont.)

T = 0.000 MS



T = 10.000 MS



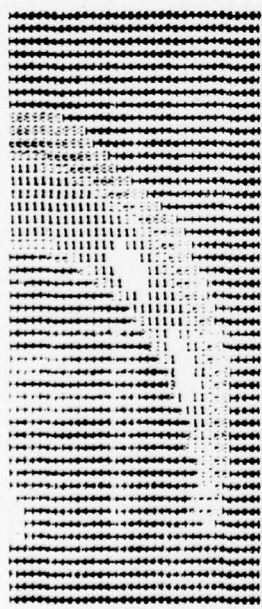
T = 24.000 MS



T = 32.000 MS



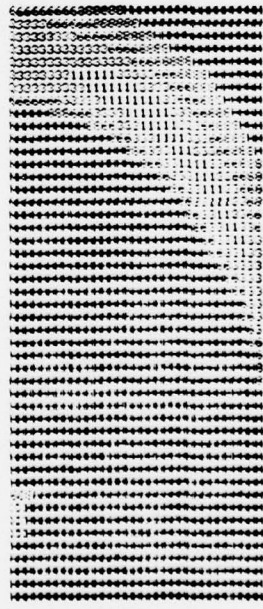
T = 40.000 MS



T = 48.000 MS



T = 56.000 MS



T = 64.000 MS

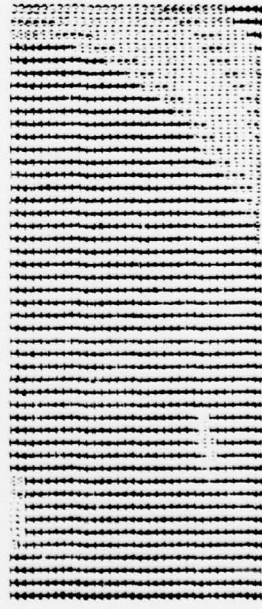


Fig. 6. Cavitation Example

Symbol	Pressure Range (m pa)
X	Structure
blank	Cavitated
1	0 - .04
3	.04 - .09
6	.09 - .14
8	.14 - .18
H	.18 - .43
A	.43 - .77
B	.77 - 1.10
C	1.10 - 1.43
D	1.43 - 1.77
E	1.77 - 2.10
F	over 2.10

Figure 7. Pressure Code

V. CONCLUSIONS AND RECOMMENDATIONS

The comparisons made between the program results where convergence of the solution has been obtained to results obtained by other methods, show that the model satisfactorily predicts the dynamic response of a ring to external pressures. The ring model cannot predict exactly the behavior of a real structure such as a submarine hull. However, by a suitable choice of ring parameters the response of the ring structure will provide a good first approximation to the response of a real structure.

A useful improvement to the program would be to include a section which would automatically pick out maximum values of bending moments and axial forces in the ring as well as when and where they occur. This would allow any desired time intervals between data printout to be used without missing peak responses.

APPENDIX

PROGRAM LISTING

STR00010
STR00020
STR00030
STR00040
STR00050
STR00060
STR00070
STR00080
STR00090
STR00100
STR00110
STR00120
STR00130
STR00140
STR00150
STR00160
STR00170
STR00180
STR00190
STR00200
STR00210
STR00220
STR00230
STR00240
STR00250
STR00260
STR00270
STR00280
STR00290
STR00300
STR00310
STR00320
STR00330
STR00340
STR00350
STR00360
STR00370
STR00380
STR00390
STR00400
STR00410
STR00420
STR00430
STR00440
STR00450
STR00460
STR00470
STR00480

XP-PRESSURES AT NODAL POINTS AT THE INSTANT OF TIME BEING EXC.
CCSINE-MATRIX OF TERMS COSINE (NPI/NNEL)
AN-FOURIER SINE COEFFICIENTS ASSOCIATED WITH RADIAL DISPL.
BN-FOURIER SINE COEFFICIENT ASSO. WITH TANGENTIAL DISPL.
ANDOT-1ST TIME DERIVATIVE OF AN
ANDOT-2ND TIME DERIVATIVE OF AN
BNDDT-1ST TIME DERIVATIVE OF BN
BNDDT-2ND TIME DERIVATIVE OF BN
NNEL-NUMBER OF ELEMENTS
NNP-NUMBER OF NODAL POINTS
XKIN-STIFFNESS COEFFICIENTS FOR FLEXURAL MOCE
XMIN-MASS COEFFICIENTS FOR FLEXURAL MODE
XKAIN-STIFFNESS COEFF. ASSO. WITH RADIAL DISPL. USED IN
*CALCULATING ANDOT
*XKBIN-STIFFNESS COEFF. ASSO. WITH TANGENTIAL DISPL. USED IN
*CALCULATING ANDOT
XMAIN-MASS COEFF. ASSO. WITH RADIAL DISPLACEMENT
XK2N-STIFFNESS COEFF. ASSO. WITH RADIAL DISPL. USED IN
*CALCULATING BNDDT
*XKB2N-STIFFNESS COEFF. ASSO. WITH TANGENTIAL DISPL. USED IN
*CALCULATING BNDDT
NNPA1-MAXIMUM NUMBER OF MODES FOR WHICH AN AND BN ARE SOLVED
*FOR SIMULTANEOUSLY
NNPA2-MAXIMUM NO. OF MODES INCLUDED IN CALCULATIONS
K1,LLL,LLL-COUNTERS
F1-TIME INCREMENT
RHO-DENSITY OF RING MATERIAL
AA-CROSS SECTIONAL AREA
RI-RADIUS OF GYRATION
R-RADIUS OF RING
E-MATERIAL MODULUS OF ELASTICITY
MM-NUMBER OF LOOPS DESIRED BETWEEN PRINTOUTS
ZN-NORMAL FORCE IN RING
ZM-BENDING MOMENT
W-RADIAL DISPLACEMENT
PH-HYDROSTATIC PRESSURE
ZFI-PI
THETA-ANGLE BETWEEN NORMAL TO SHOCK FRONT AND LOCATION ON RING

SUBROUTINE INPUT

IMPLICIT REAL*8 (A-H,O-Z)
COMMON/OUT/K(20)
COMMON/SINT/NNEL, NNP, MM, NN, NNPA1N, NNPA2N, L, LLL

CC


```

COMMON/REAL/HH,AA,E,R,RI,RHO,GC,TI
COMMON/VECTORS/XP(50),COSINE(50),ANDDT(50),BN(50)
*,BNDOT(50),ANDOT(50),BNDOT(50),XKAIN(50),XMAIN(50),AN(50)
*,XKA2N(50),XKBIN(50),XKB2N(50),CN(50),XMIN(50),XKIN(50)
COMMON/IPASS/DT,A,PH,N
COMMON/SPASS/PASS(50)

```

C READ NEEDED CONSTANTS

```

ZPI=4.DO*DATAV(1.DO)
NNP=4*N+1
NNEL=NNP-1
HF=DT
R=A
L=0
READ(5,26)MM
READ(5,27)AA,E,RI,RHO
FORMAT(6I5)
FCRMAT(7G10.3)
EXTN=2*ZPI*R/((5*DT)*(E/RHO)**.5)
FLEXN=(EXTN*R/RI)**.5
NNPAIN=EXTN
NNPA2N=FLEXN
IF(NNP.LT.NNPAIN)NNPAIN=NNP
IF(NNP.LT.NNPA2N)NNPA2N=NNP
RETURN
END

```

26

27

32

SUBROUTINE COEFF1

```

IMPLICIT REAL*8(A-H,O-Z)
COMMON/SINT/NNEL,NNP,MM,NN,NNPAIN,NNPA2N,L,LLL
COMMON/REAL/HH,AA,E,R,RI,RHO,GC,TI
COMMON/VECTORS/XP(50),COSINE(50),ANDDT(50),BN(50)
*,ANDDT(50),ANDOT(50),BNDOT(50),XKAIN(50),XMAIN(50),AN(50)
*,XKA2N(50),XKBIN(50),XKB2N(50),CN(50),XMIN(50),XKIN(50)
COMMON/IPASS/DT,A,PH,N

```

```

RI=R/RI/R
EAKS=E*AA/(R*R)
RA=RHO*AA
ECRHS=E/(RHO*R**2)
Z=RI**2
ZPI=4.DO*DATAV(1.DO)

```

C FORM FOURIER COEFFICIENTS FOR PRESSURE REPRESENTATION AND

```

STR00490
STR00500
STR00510
STR00520
STR00530
STR00540
STR00550
STR00560
STR00570
STR00580
STR00590
STR00600
STR00610
STR00620
STR00630
STR00640
STR00650
STR00660
STR00670
STR00680
STR00690
STR00700
STR00710
STR00720
STR00730
STR00740
STR00750
STR00760
STR00770
STR00780
STR00790
STR00800
STR00810
STR00820
STR00830
STR00840
STR00850
STR00860
STR00870
STR00880
STR00890
STR00900
STR00910
STR00920
STR00930
STR00940
STR00950
STR00960

```

STR00970
STR00980
STR00990
STR01000
STR01010
STR01020
STR01030
STR01040
STR01050
STR01060
STR01070
STR01080
STR01090
STR01100
STR01110
STR01120
STR01130
STR01140
STR01150
STR01160
STR01170
STR01180
STR01190
STR01200
STR01210
STR01220
STR01230
STR01240
STR01250
STR01260
STR01270
STR01280
STR01290
STR01300
STR01310
STR01320
STR01330
STR01340
STR01350
STR01360
STR01370
STR01380
STR01390
STR01400
STR01410
STR01420
STR01430
STR01440

FORM MASS AND STIFFNESS COEFFICIENTS

```

DC 500 I=1, NNP
XI=I
DO 505 J=1, NNP
XJ=J
XNEL=NNEL
T=PI*(XJ-1.D0)*(XJ-1.D0)*ZPI/XNEL
COSINE(I,J)=DCOS(THETA)
CONTINUE
XI=XI-1.D0
XMAIN(I)=RA*(1.D0+Z**XI**2)
XKAIN(I)=EAORS*(Z**XI**2-1.D0)**2+1.D0)
X*BLN(I)=EACRS*XJ
XKA2N(I)=EORHS*XJ**2
XKB2N(I)=EORHS*XJ**2
IF(I.EQ.1)GC TO 582
XMIN(I)=RA*(1.D0+Z**XI**2+1.D0)/XI**2+Z**XI**2)
XKIN(I)=EAORS*(RIR**2*(XI**2-1.D0)**2)
CONTINUE
CALL PRINT2(14)

```

SET COEFFICIENTS = 0 INITIALLY

```

PH=PH/XKAIN(I)
DO 526 I=1, NNP
AN(I)=0.D0
ANDOT(I)=0.D0
BNDOT(I)=0.D0
EN(I)=0.D0
AN(I)=PH
LLL=1
TI=0.D0
L=1
RETURN
END

```

SUBROUTINE TIMSTP

```

IMPLICIT REAL*8(A-H,O-Z)
COMMON/SINT/NNEL,NNP,MM,NN,NNPA1N,NNPA2N,L,LLL
COMMON/REAL/HH,AA,E,R,R1,RHO,GC,TI

```

```

CALL PINPUT
CALL CNS
TI=LLL*HH
CALL PREDIC
CALL MOMFOR

```

STR01450
STR01460
STR01470
STR01480
STR01490
STR01500
STR01510
STR01520
STR01530
STR01540
STR01550
STR01560
STR01570
STR01580
STR01590
STR01600
STR01610
STR01620
STR01630
STR01640
STR01650
STR01660
STR01670
STR01680
STR01690
STR01700
STR01710
STR01720
STR01730
STR01740
STR01750
STR01760
STR01770
STR01780
STR01790
STR01800
STR01810
STR01820
STR01830
STR01840
STR01850
STR01860
STR01870
STR01880
STR01890
STR01900
STR01910
STR01920

```

CALL DISPLA
L=L+1
LLL=LLL+1
RETURN
STOP
END

SUBROUTINE PINPUT

IMPLICIT REAL*8(A-H,O-Z)
COMMON/SINT/NNEL,NNP,MM,NN,NNPAIN,NNPA2N,L,LLL
COMMON/REAL/HH,AA,E,R,RI,RHO,GC,TI
COMMON/VECTS/XP(50),COSINE(50,50),ANDDT(50),BN(50)
*,BNDDT(50),ANDDT(50),BNDDT(50),XKAIN(50),XMAIN(50),AN(50)
*,XKA2N(50),XKBIN(50),XKB2N(50),CN(50),XMIN(50),XKIN(50)
COMMON/SPASS/PASS(50)
FORMAT(16G10.2)
DO 6 I=1,NNP
XP(I)=PASS(I)
XP(1)=XP(1)/2.00
XP(NNP)=XP(NNP)/2.00
CALL PRINT2(15)
RETURN
END

SUBROUTINE CNS

IMPLICIT REAL*8(A-H,O-Z)
COMMON/SINT/NNEL,NNP,MM,NN,NNPAIN,NNPA2N,L,LLL
COMMON/REAL/HH,AA,E,R,RI,RHO,GC,TI
COMMON/VECTS/XP(50),COSINE(50,50),ANDDT(50),BN(50)
*,BNDDT(50),ANDDT(50),BNDDT(50),XKAIN(50),XMAIN(50),AN(50)
*,XKA2N(50),XKBIN(50),XKB2N(50),CN(50),XMIN(50),XKIN(50)

C SOLVE FOR CN'S
DC 60 I=1,NNP
C=0.00
DC 65 J=1,NNP
C=XP(J)*COSINE(I,J)+C
CONTINUE
XNEL=NNEL
CN(I)=(2.00/XNEL)*C
IF(1.EQ.1)CN(I)=CN(I)/2.00

```

76

5
6

C
65

STR01930
STR01940
STR01950
STR01960
STR01970
STR01980
STR01990
STR02000
STR02010
STR02020
STR02030
STR02040
STR02050
STR02060
STR02070
STR02080
STR02090
STR02100
STR02110
STR02120
STR02130
STR02140
STR02150
STR02160
STR02170
STR02180
STR02190
STR02200
STR02210
STR02220
STR02230
STR02240
STR02250
STR02260
STR02270
STR02280
STR02290
STR02300
STR02310
STR02320
STR02330
STR02340
STR02350
STR02360
STR02370
STR02380
STR02390
STR02400

IF(I.EQ.NNP)CN(I)=CN(I)/2.D0
CONTINUE
RETURN
END

60

SUBROUTINE PREDIC

IMPLICIT REAL*8(A-H,O-Z)
COMMON/INT/NNEL,NNP,MM,NN,NNPA,NNPA2N,L,LLL
COMMON/REAL/HH,AA,E,R,RHO,GC,T
COMMON/VECT S/XP(50),COSINE(50),ANDDT(50),BN(50)
*,BNDDT(50),ANDDT(50),XKALN(50),XKALN(50),AN(50)
*,XKA2N(50),XKB1N(50),XKB2N(50),CN(50),XMIN(50),XK1N(50)

C CENTRAL DIFFERENCE INTEGRATION OF D.E. TO PREDICT FUTURE AIN'S

IF(LLL.NE.1)GO TO 541
DO 542 I=1,NNP
IF(I.GT.NNPA2N)GO TO 542
IF(I.GT.NNPAIN)GO TO 543
ANDDT(I)=(CN(I)-XKALN(I))*AN(I)-XKB1N(I)*BN(I))/XMAIN(I)
ANDDT(I)=-.500*ANDDT(I)*HH
BNDDT(I)=-.500*ANDDT(I)*BN(I)
BNDDT(I)=-.500*BNDDT(I)*HH
GO TO 542

543

542
541

ANDDT(I)=(CA(I)-AN(I)*XK1N(I))/XMIN(I)
ANDDT(I)=-.500*ANDDT(I)*HH
CONTINUE
DO 540 I=1,NNP
IF(I.GT.NNPAIN)GO TO 550
XI=I
ANDDT(I)=(CN(I)-XKALN(I))*AN(I)-XKB1N(I)*BN(I))/XMAIN(I)
ANDDT(I)=ANDDT(I)+ANDDT(I)*HH
AN(I)=AN(I)+ANDDT(I)*HH
BNDDT(I)=-.500*ANDDT(I)*AN(I)+XKB2N(I)*BN(I)
BNDDT(I)=BNDDT(I)+BNDDT(I)*HH
BN(I)=BN(I)+BNDDT(I)*HH
GO TO 540

550

CONTINUE
IF(I.GT.NNPA2N)GO TO 540
ANDDT(I)=(CN(I)-AN(I)*XK1N(I))/XMIN(I)
ANDDT(I)=ANDDT(I)+HH*ANDDT(I)
AN(I)=AN(I)+HH*ANDDT(I)
XI=I-1
BN(I)=-AN(I)/XI
CONTINUE

540

CALL PRINT2 (17)
RETURN
ENC

SUBROUTINE MOMFOR

```

IMPLICIT REAL*8(A-H,O-Z)
COMMON/DIS/W(50)
COMMON/SINT/NNEL,NNP,MM,NN,NNPA1N,NNPA2N,L,LLL,LLLL,J
COMMON/REAL/HH,AA,E,R,RHO,GC,TI,ZN,ZM
COMMON/VECTS/XP(50),CSINE(50,50),ANDDT(50),BN(50)
*,BNDOT(50),ANDDT(50),XKAIN(50),XMAIN(50),AN(50)
*,XKA2N(50),XKB1N(50),XKB2N(50),CN(50),XMIN(50),XKIN(50)

```

C CALCULATE BENDING MOMENTS AND AXIAL FORCE

```

ZPI=4.DC*DATAV(1.D0)
Z=(RI/R)**2
LLLL=1
C=-E*AA*R I**2/R**2
B=E*AA/R
DO 601 J=1,NNP
  ZM=0.D0
  ZN=0.D0
  DO 602 I=1,NNP
    XI=I-1
    XJ=J-1
    ZM=C*(1-XI**2)*AN(I)*DCOS(XI*XJ*ZPI/NNEL)+ZP
    ZN=-B*(AN(I)*(1+Z*(1-XI**2))+XI*BN(I))*DCOS(XI*XJ*ZPI/NNEL)+ZN
  CALL PRINT2 (16)
  LLLL=1
RETURN
END

```

602
601

SUBROUTINE DISPLA

```

IMPLICIT REAL*8(A-H,O-Z)
COMMON/DIS/W(50)
COMMON/SINT/NNEL,NNP,MM,NN,NNPA1N,NNPA2N,L,LLL
COMMON/REAL/HH,AA,E,R,RHO,GC,TI,ZN,ZM
COMMON/VECTS/XP(50),CSINE(50,50),ANDDT(50),BN(50)
*,BNDOT(50),ANDDT(50),XKAIN(50),XMAIN(50),AN(50)
*,XKA2N(50),XKB1N(50),XKB2N(50),CN(50),XMIN(50),XKIN(50)
COMMON/SPASS/PASS(50)

```

STR02410
STR02420
STR02430
STR02440
STR02450
STR02460
STR02470
STR02480
STR02490
STR02500
STR02510
STR02520
STR02530
STR02540
STR02550
STR02560
STR02570
STR02580
STR02590
STR02600
STR02610
STR02620
STR02630
STR02640
STR02650
STR02660
STR02670
STR02680
STR02690
STR02700
STR02710
STR02720
STR02730
STR02740
STR02750
STR02760
STR02770
STR02780
STR02790
STR02800
STR02810
STR02820
STR02830
STR02840
STR02850
STR02860
STR02870
STR02880


```

26      FORMAT(6I5)
      WRITE(6,1010)
1010    FORMAT(/,6X,'I',8X,'XKAIN',8X,'XKA2N',8X,'XMAIN',8X,'XKBIN')
      WRITE(6,1015)(I,XKAIN(I),XKA2N(I),XMAIN(I),XKBIN(I),
      *I=1,NNP)
1015    FORMAT(18,2X,4G13.5)
      RETURN

C      PRINT INPUT PRESSURE

15      WRITE(6,75)
      XP(1)=XP(1)*2.00
      XP(NNP)=XP(NNP)*2.00
      FCRMAT(/,3X,'NODAL POINT PRESSURES',/)
      WRITE(6,51)(XP(I),I=1,NNP)
      XP(1)=XP(1)/2.00
      XP(NNP)=XP(NNP)/2.00
      FCRMAT(6G10.2)
      RETURN

C      PRINT BENDING MOMENTS & AXIAL FORCES

16      IF(LLLL.NE.1)GO TO 606
      LLLL=LLLL+1
      WRITE(6,604)
      FCRMAT(/,6X,'NP
      WRITE(6,603)J,ZM,ZN
      FCRMAT(3X,15,8X,615.5,8X,615.5)
      RETURN

C      PRINT TIME, AN,BN, & CN

17      WRITE(6,70) T1
70      FORMAT(/,3X,'TIME =',3PF8.3,' MS')
      WRITE(6,1020)
      FCRMAT(/,2X,
      *BN
1020    WRITE(6,1000)(BN(I),AN(I),CN(I),I=1,NNP)
      FCRMAT(3G15.5)
      RETURN

C      PRINT NODAL POINT DISPLACEMENTS

```

FORCE',/)

CN')

```

18      WRITE(6,80)
35      WRITE(6,35) (I,W(I),I=1,NNP)
80      FORMAT(15,12X,G15.5)
      FFORMAT(1,12X,GP) NODAL POINT DISPLACEMENTS',/,)
      L=0
      RETURN
      END

```

```

STR03850
STR03860
STR03870
STR03880
STR03890
STR03900
STR03910
STR03920
STR03930

```

LIST OF REFERENCES

1. Newton, R.E., "Effects of Cavitation on Underwater Shock Loading - Part 1," NPS-69-78-013, Naval Postgraduate School, Monterey, CA, July 1978.
2. Newton, R.E., "Effects of Cavitation on Underwater Shock Loading - Plane Problem, Part I," NPS-69-79-007PR, Naval Postgraduate School, Monterey, CA, July 1979.
3. Timoshenko, S., Strength of Materials, Part I. New York: D. Van Nostrand Company, Inc., 1955.
4. Timoshenko, S., Theory of Plates and Shells. New York: McGraw-Hill Book Company, Inc., 1959.
5. Newton, R.E., "Some Matrix Applications to Vibration Problems," Class Notes, Naval Postgraduate School, Jan. 1975.
6. Roark, R.J., and Young, W.C., Formulas For Stress And Strain, New York: McGraw-Hill Book Company, 1975.

INITIAL DISTRIBUTION LIST

	No. Copies
1. Defense Documentation Center Cameron Station Alexandria, Virginia 22314	2
2. Library, Code 0142 Naval Postgraduate School Monterey, California 93940	2
3. Department Chairman, Code 69 Department of Mechanical Engineering Naval Postgraduate School Monterey, California 93940	2
4. Professor. R. E. Newton, Code 69Ne Department of Mechanical Engineering Naval Postgraduate School Monterey, California 93940	5
5. Jack T. Waller Jr., Code 3354 FUZE Department Naval Weapons Center China Lake, California 93555	1
6. Dr. Eugene Sevin SPSS Defense Nuclear Agency Washington, D. C. 20305	1
7. Dr. Gordon C. Everstine, Code 1844 David W. Taylor Naval Ship Research and Development Center Bethesda, Maryland 20084	1
8. Commander Naval Weapons Center China Lake, California 93555 ATTN: Code 533 (Tech Lib)	1
9. Dr. Melvin L. Baron Weidlinger Associates 110 East 59th Street New York, New York 10022	1
10. Dr. Thomas L. Geers Dept. 52-33/Bldg. 205 Lockheed Palo Alto Research Laboratory 3251 Hanover Street Palo Alto, California 94304	1